

Proceedings of the ASME 2018 16th International Conference on Nanochannels, Microchannels, and Minichannels ICNMM2018 June 10-13, 2018, Dubrovnik, Croatia

ICNMM2018-7690

INVESTIGATION OF IN-AIR DROPLET GENERATION IN CONFINED PDMS MICROCHANNELS OPERATING IN THE JETTING REGIME

Pooyan Tirandazi

Northeastern University Boston, Massachusetts, USA

Julian D. Arroyo

Northeastern University Boston, Massachusetts, USA

John Healy

Northeastern University Boston, Massachusetts, USA

Carlos H. Hidrovo

Northeastern University Boston, Massachusetts, USA

ABSTRACT

Liquid-in-air generation of monodisperse, microscale droplets is an alternative to conventional liquid-in-liquid methods. Previous work has validated the use of a highly inertial gaseous continuous phase in the production of monodisperse droplets in the dripping regime using planar, flow-focusing, PDMS microchannels. The jetting flow regime, characteristic of small droplet size and high generation rates, is studied here in novel microfluidic geometries. The region associated with the jetting regime is characterized using the liquid Weber number (We_l) and the gas Reynolds number (Re_g) . We explore the effects of microchannel confinement on the development and subsequent breakup of the liquid jet as well as the physical interactions between the jet and continuous gaseous flow. Droplet breakup in the jetting regime is also studied numerically and the influence of different geometrical parameters is investigated. Numerical simulations of the jetting regime include axisymmetric cases where the jet diameter and length are studied. This work represents a vital investigation into the physics of droplet breakup in the jetting regime subject to a confined gaseous co-flow. By understanding the effects that different flow and geometry conditions have on the generation of droplets, the use of this system can be optimized for specific high-demand applications in the aerospace, material, and biological industries.

INTRODUCTION

The controlled breakup of a liquid jet to form microscale fluid entities has been extensively studied over the past 30 years because of its significance in a multitude of applications such as material synthesis and pharmaceutical drugs [1]–[3]. In comparison to the dripping regime, the jetting regime enables the

generation of smaller droplets that are commensurate to the jet size at higher frequencies [4]. These benefits are usually achieved at the expense of monodispersity of the generated droplets [5]. Recent advances in microfluidic techniques have catalyzed the ability to form monodisperse droplets from jet breakup inside microchannels [6]. In the microfluidic literature, production of droplets usually involves a secondary viscous liquid such as an oil phase, to drive the jet breakup [7], [8]. Many studies therefore, have investigated the confined coflowing liquid streams to better understand the jet behavior and control the breakup. Using air as the continuous phase is a newer alternative to conventional droplet-based microfluidic systems [9]–[12]. We have recently reported a droplet microfluidic device that uses a high-speed gaseous flow as the continuous phase to facilitate breakup of a fluid jet in confined PDMS microchannels. Previous investigations in this regard have demonstrated the potential of such platform, with results showing droplet generation rates in the order of 10⁵ drop/s from a liquid jet inside the microchannel [13]. Despite the vast literature on the study of a liquid jet in confined liquid flows [14]–[18], no study has addressed the question of coflowing liquid in confined gas flows. The studies that have investigated the liquid jet breakup in a coaxial gas stream, consider the jet discharching into an open environment at atmospheric pressure [19], [20]. Therefore, little is known about the jet behavior when subject to a confined gas flow. Improvements in the production of uniform particles using this method cannot be done without a good understanding of jet dynamics at the microscopic scale. In this work, we study the formation and breakup of a liquid jet in a coaxial gas stream inside a microchannel (Figure 1). We experimentally characterize the jet behavior in terms of relevant dimensionless numbers. A numerical simulation study is also presented to further investigate the effect of different parameters

on these microfluidic jets. The results of this work are useful for improving the performance of droplet generation using the jetting regime which can be applied to high throughput generation of uniform aerosols and particles using compact microfluidic devices.

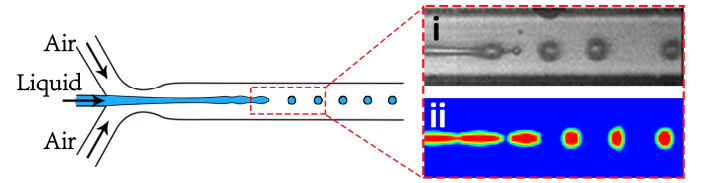


Figure 1. Schematic view of the microfluidic droplet generation studied in this work operating in the jetting regime. (i) Experimental image of the microjet inside the microchannel, (ii) numerical simulations of the jet and a co-axial confined gaseous flow.

EXPERIMENTAL

Experiments are performed inside PDMS microchannels with a flow-focusing geometry. The microchannel network is made by Photolithography on multiple layers of SU-8 and soft lithography for device replication. Detailed fabrication procedure as well as the experimental setup has been explained in a previous work [13]. Compressed air (ρ =1.225 kg/m³ and μ =1.78×10⁻⁵ Pa.s) is used as the continuous phase and DI water (ρ =998 kg/m³ and μ =0.001 Pa.s) as the dispersed phase.

The jetting regime is characterized by the gas Reynolds number (Re_g) and liquid Weber number (We_l);

$$Re_g = \frac{\rho U D_h}{\mu}, \quad We_l = \frac{\rho U^2 D_{h,l}}{\sigma}$$
 (1)

These numbers describe, respectively, the ratio of the inertia to viscous forces of the continuous air phase, and the inertia forces of the liquid phase compared to the surface tension forces. ρ and U in each equation represent the density and velocity of the corresponding phase. μ is the air viscosity and σ is the interfacial tension between air and water. D_h represents the hydraulic diameter of the microchannel outlet, whereas $D_{h,l}$ is the hydraulic diameter of the liquid inlet. Figure 2 shows the parameter window where the jetting regime is observed inside the microchannel.

Unlike typical microfluidic systems in which inertia is neglected due to the low Reynolds numbers [21], the values for Re_g vary from 200 to 750 within the jetting regime of this system. Therefore, the effects of air inertia in the gas-liquid jetting regime can be considered significant. Instead of considering the Capillary number of the continuous phase [22], we characterize the jetting in terms of the gas Reynolds number to capture these physics better. We observe that dripping-to-jetting transition occurs for $We_l > 0.6$. Jetting process starts once the inertia of the liquid phase balances the surface tension forces. In this state, the liquid is stretched into the microchannel and creates the jet. Breakup of the droplets from the jet is governed by the Raleigh-Plateau instability [23]. We observed that at high Re_g the jet starts

to oscillate inside the microchannel due to highly inertial flow of the air.

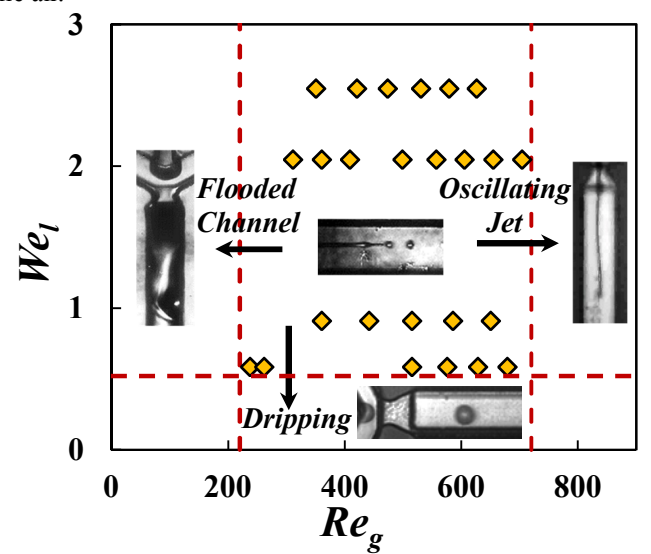


Figure 2. Representation of the parameter window for jetting region under different Re_g and Wei.

Early studies on the breakup of liquid jets in both liquid and gaseous media characterized the most unstable mode of the Rayleigh-Plateau to be proportional to the jet diameter. Therefore, understanding how flow and geometry conditions effect the jet diameter opens new opportunities for understanding the underlying physics of the jetting regime. After the initial meniscus, the extended jet ultimately reaches a relatively constant diameter. We measured the jet diameter inside the microchannel for different channel hydraulic diameters. The measurements are done using ImageJ software. Figure 3 shows the jet diameter over the hydraulic diameter of the microchannel (d_1/D_h) for two different channels over the Re_g .

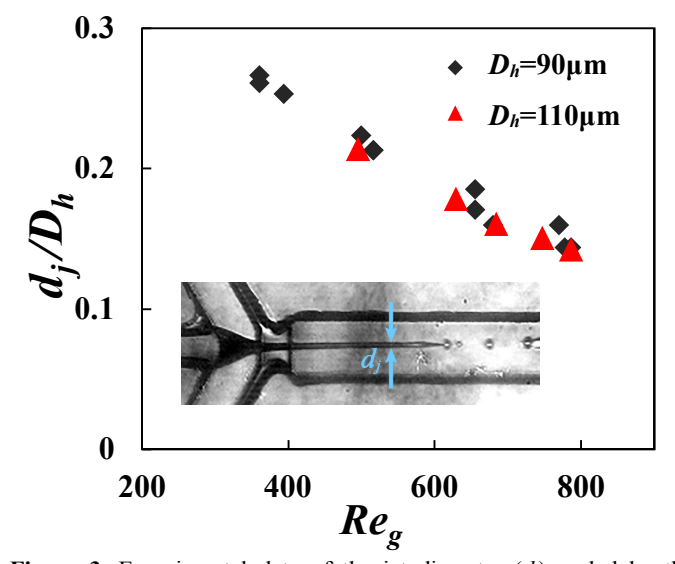


Figure 3. Experimental data of the jet diameter (d_j) scaled by the hydraulic diameter of the microchannel (D_h) as a function of the gas Reynolds number (Re_g) .

As the Re_g increase, due to higher inertia forces of the air, jet size decreases. We tested two different microchannels with 90 μ m and 101 μ m hydraulic diameter, and the results show that that jet diameter holds a direct relationship with microchannel confinement size. Therefore, formation of smaller jets is possible by fabricating smaller channel sizes.

NUMERICAL SIMULATION

By employing numerical simulation techniques, the jetting regime and its relationship with flow and geometrical conditions can be studied more comprehensively. Although the ability to monitor critical metrics through the flow is attractive. Proper representation of the two-phase system must be ensured.

Several computational methods are used in the simulation and tracking of two-phase systems. Of the existing methods, Level Set (LS) and Volume-of-Fluid (VOF) are the most commonly implemented in the simulation of liquid-gas interfaces [24]. While both methods solve a scalar function to determine the position of the phase interface, the mechanism by which these methods construct the interface is different. VOF solves for the volume fraction and spatial domain of the secondary phase in each cell. This method inherently conserves the mass, but lacks in fidelity when computing the interface boundary location. The LS method on the other hand, assigns a level set function to the interface, allowing for accurate tracking of the boundary position at the cost of the computation time [25].

Reliable tracking of the interface in simulation of the gasliquid systems, specifically in the jetting regime, is paramount. Proper representation of interface curvatures ensures that droplet detachment by Raleigh-Plateau instability occurs accurately. For this reason, this paper utilizes the coupled level set and volume of fluid method (CLSVOF), to overcome the shortfalls of each individual technique. Simulations were performed in ANSYS Fluent (Ver. 18.2, ANSYS, USA). The software solves the governing equations of the system together with the CLSVOF method. The governing equations of both phases include continuity Equation and the momentum equation

$$\frac{\partial \rho}{\partial t} + \nabla \rho U = 0 \tag{2}$$

$$\frac{\partial(\rho U)}{\partial t} + \nabla(\rho U^2) = -\nabla p + \nabla \mu [(\nabla U + (\nabla U)^{\mathrm{T}}] + F_{\sigma}$$
 (3)

where U is the velocity vector, ρ is the density, μ is the kinematic viscosity, p is the pressure, and F_{σ} is the surface tension of the phase interface. In this paper surface tension forces between water and air were modeled as 0.072 N/m, implemented by the Continuum Surface Force (CSF) method [26] detailed in equation 4

$$F_{\sigma} = \sigma \kappa(\varphi) \nabla(\varphi) \tag{4}$$

where κ is the curvature of the interface as defined by

$$\kappa(\varphi) = \nabla \cdot \frac{\nabla \varphi}{|\nabla \varphi|} \tag{5}$$

The level set equation [25] is solved in conjunction with the continuity and momentum equations and is defined as

$$\frac{d\varphi}{dt} + U \cdot \nabla \varphi = 0 \tag{6}$$

$$\phi(x,t) = \begin{cases}
d, & \text{if } x \text{ is in the liquid phase} \\
0, & \text{if } x \text{ is on the interface} \\
-d, & \text{if } x \text{ is in the gas phase}
\end{cases} (7)$$

where φ is the level set function, x is the position vector of the interface, and d is the minimum distance of the interface at time t. This level set function is then coupled with the following equations of the VOF function.

$$\frac{\partial \alpha_g}{\partial t} + U \cdot \nabla \alpha_g = 0 \tag{8}$$

$$\frac{\partial \alpha_l}{\partial t} + U \cdot \nabla \alpha_l = 0 \tag{9}$$

 α_g and α_l represent the volume fraction of the gas and liquid phases in the cell respectively.

A simple axisymmetric co-flow geometry was chosen to investigate the jetting regime in a confined, gas flow to gain a better understanding of the mechanisms associated with droplet detachment. Droplet generation characteristics in this geometry were validated against experimental results for droplet diameter and generation frequency, showing less than 10% deviation between the two cases.

The simulation geometry was modeled with the experimental value of the hydraulic diameter of the outlet channel as the confinement diameter. The liquid inlet was oriented in the center of this confinement, with the gas inlet being the annular area between the liquid inlet and confinement wall. Both inlet boundary conditions were set as a constant velocity inlet. The outlet of the channel was set as an atmospheric pressure outlet boundary. The walls were assigned no-slip boundary conditions and a contact angle of 110°. Figure 4 represents the details of the simulation domain along with the boundary conditions.

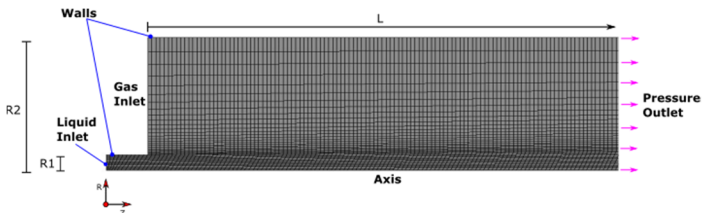


Figure 4. Schematic of the numerical grid for the simulation studies.

Structured quadrilateral elements were used to mesh the geometry. The grid was refined in areas of phase interface movement and was checked for independence. Simulation time steps were adjusted to ensure convergence and maintain a global courant number of less than unity. For the reported results, this was 10^{-8} seconds, with first order implicit time stepping of the unsteady term.

We have run the simulations for two different microchannels with $10\mu m$ and $20\mu m$ liquid inlet, while the rest of the dimensions are kept the same. For each geometry Re_g and We_l are varied over two orders of magnitude to distinguish the influence of the altered parameter. Figure 5 shows sequences of jet formation inside the microchannel obtained from numerical simulations. Jetting in the simulations happens at $We_l > 1$ which is close to the experimental observations.

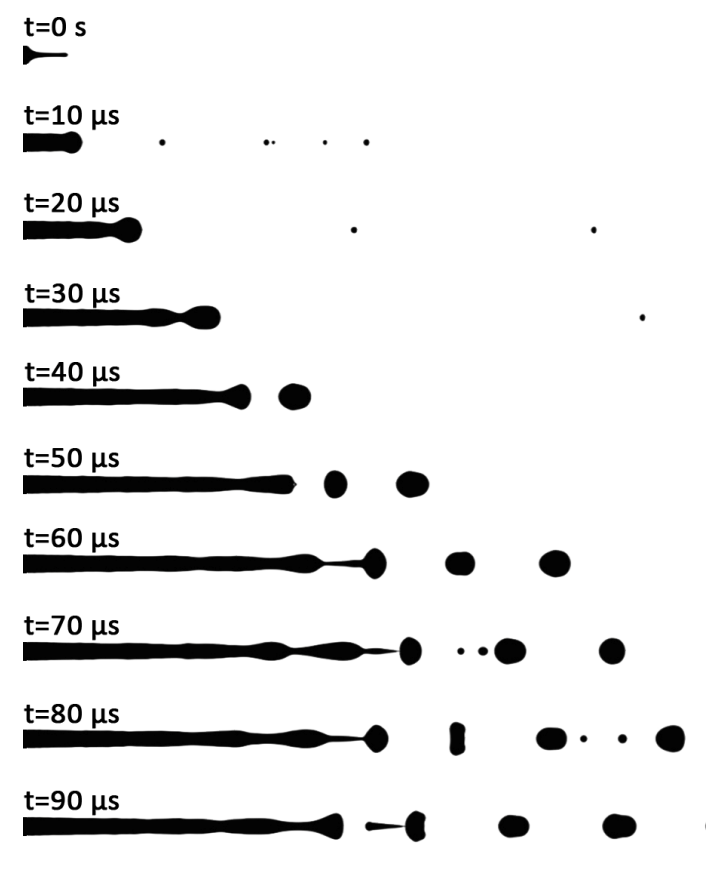


Figure 5. Consequential simulation images of the formation of the jet in a confined co-axial gas flow. The walls of the microchannel are not shown here. The dimensionless numbers for the above images are set as Re_g =500 and We_F =10.

We investigated the jet length (L_j) as a function of Re_g and We_l . L_j is defined as the distance where the droplet breakup happens. Figure 6 shows the jet length which is scaled by the hydraulic diameter of the microchannel (D_h) . As the We_l increases, the inertia of liquid forces the jet to extend more into the microchannel. Increasing Re_g creates a bigger inertial drag on the liquid which also elongates the jet. At low We_l the jet length

is close to zero which represents the transition to the dripping regime where the breakup is occurring at the exit of the liquid channel. We also investigated the effect of the liquid channel inlet on the jet size. We used a liquid inlet size of $D_{h,l}=10\mu m$ and $D_{h,l}=20\mu m$. Figure 7 shows the jet diameter (d_j) for the two different liquid inlet sizes as the Re_g increases. The jet size is scaled by the liquid inlet size $(D_{h,l})$. Starting at lower Re_g the liquid jet is similar the inlet size, as the Re_g increase, the jet profile shrinks as it moves downstream and reaches a relatively constant value that is smaller than the inlet size. Decreasing the inlet size results in thinner jets. It should be noted that we did not find a substantial difference on the jet diameter by varying the We_l . However, as We_l is increased, longer jets are generated.

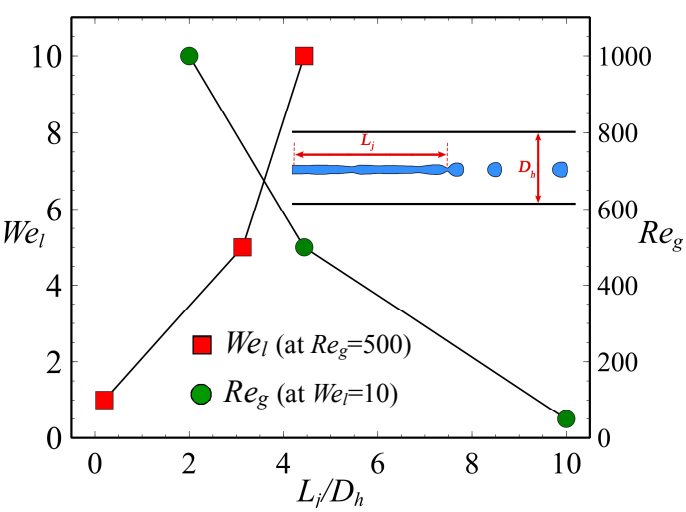


Figure 6. The jet length in confined coaxial flow of gas for different gas Reynolds numbers (Re_g) and liquid weber numbers (We_l).

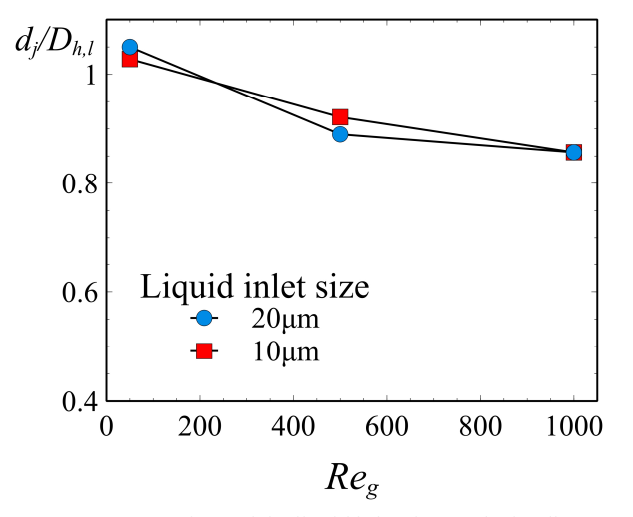


Figure 7. Comparison of the liquid inlet size on the jet diameter for two different cases ($10\mu m$ and $20\mu m$). The jet diameter is proportionally reduced as the inlet size becomes smaller.

CONCLUSIONS

In this paper, we experimentally and numerically study the formation and characteristics of a liquid microjet inside a confined microchannel subject to high speed gaseous flows. For the experimental part, we use a flow-focusing microfluidic device fabricated in PDMS. We consider the parameter space over which the jetting regime resides in terms of the gas Reynolds number (Re_g) and liquid Weber number (We_l) . The jet diameter is characterized as a function of Re_g for two different microchannel sizes. Results show it is possible to obtain smaller jets in confined liquid-gas co-flows by decreasing the microchannel scale. In the numerical section, we simulate the jetting process in a simple co-flow geometry. The jet length is defined as the breakup distance of the droplets and is characterized for different Re_g and We_l . Finally, we consider two different liquid channel inlets and measure the jet diameter in each case.

The results of this work can be useful for understanding the conditions that produce ultrasmall jets. Under such conditions, small droplets and particles in the order of micron may be generated using the presented microfluidic approach. Using the gas as the continuous phase ensure the cleanness of the generated particles. Moreover, a liquid-in-gas approach can produce droplet at much faster rates in comparison to a liquid-in-liquid microfluidic system. Therefore, this system can be implemented for large scale production of submicron particles which suitable for pharmaceutical and material industries.

NOMENCLATURE

 $\mu = \text{viscosity}, \text{Pa.s}$

 $\rho = \text{Density, kg.m}^{-3}$

 $U = \text{Velocity, m.s}^{-1}$

 $\sigma = \text{Air-water surface tension, N.m}^{-1}$

 $Re_g = Gas Reynolds number$

 We_l = Liquid Weber number

 d_i = Jet diameter, m

 L_i = Jet length, m

 D_h = Hydraulic diameter of the outlet, m

 $D_{h,l}$ = Hydraulic diameter of the liquid channel, m

ACKNOWLEDGMENTS

This work has been funded with an NSF CAREER Award grant CBET-1522841.

REFERENCES

- [1] L. Shang, Y. Cheng, and Y. Zhao, "Emerging Droplet Microfluidics," *Chem. Rev.*, vol. 117, no. 12, pp. 7964–8040, 2017.
- [2] Q. Xu *et al.*, "Preparation of monodisperse biodegradable polymer microparticles using a microfluidic flow-focusing device for controlled drug delivery," *Small*, vol. 5, no. 13, pp. 1575–1581, 2009.
- [3] R. Seemann, M. Brinkmann, T. Pfohl, and S. Herminghaus, "Droplet based microfluidics," *Reports*

- Prog. Phys., vol. 75, no. 1, p. 16601, 2012.
- [4] J. K. Nunes, S. S. H. Tsai, J. Wan, and H. a Stone, "Dripping and jetting in microfluidic multiphase flows applied to particle and fiber synthesis.," *J. Phys. D. Appl. Phys.*, vol. 46, no. 11, p. 114002, 2013.
- [5] F. Cruz-Mazo, J. M. Montanero, and A. M. Gañán-Calvo, "Monosized dripping mode of axisymmetric flow focusing," *Phys. Rev. E Stat. Nonlinear, Soft Matter Phys.*, vol. 94, no. 5, pp. 1–5, 2016.
- [6] P. Zhu and L. Wang, "Passive and active droplet generation with microfluidics: a review," *Lab Chip*, vol. 17, no. 1, pp. 34–75, 2016.
- [7] T. Cubaud and T. G. Mason, "Capillary threads and viscous droplets in square microchannels," *Phys. Fluids*, vol. 20, no. 5, p. 53302, 2008.
- [8] S. L. Anna, "Droplets and Bubbles in Microfluidic Devices," *Annu. Rev. Fluid Mech.*, vol. 48, no. 1, pp. 285–309, 2016.
- [9] P. Tirandazi and C. H. Hidrovo, "Liquid-in-gas droplet microfluidics; experimental characterization of droplet morphology, generation frequency, and monodispersity in a flow-focusing microfluidic device," *J. Micromechanics Microengineering*, vol. 27, no. 7, 2017.
- [10] P. Tirandazi and C. H. Hidrovo, "Experimental Investigation of Geometrical Parameters for Gas-Liquid Droplet Generation In Flow-Focusing Configurations," in ASME 2015 13th International Conference on Nanochannels, Microchannels, and Minichannels ICNMM15, 2015, pp. 1–6.
- [11] P. Tirandazi and C. H. Hidrovo, "Generation of Uniform Liquid Droplets in A Microfluidic Chip Using A Highspeed Gaseous Microflow," in *Proceedings of the ASME 2016 14th Conference on Nanochannels, Microchannels, and Minichannels ICNMM2016*, 2016, pp. 1–6.
- [12] A. Shahriari, M. M. Kim, S. Zamani, N. Phillip, B. Nasouri, and C. H. Hidrovo, "Flow regime mapping of high inertial gas-liquid droplet microflows in flow-focusing geometries," *Microfluid. Nanofluidics*, vol. 20, no. 1, p. 20, 2016.
- [13] P. Tirandazi, G. Tomic, and C. H. Hidrovo, "An Ultra-High-Throughput Flow-Focusing Microfluidic Device for Creation of Liquid Droplets in Air," no. 58301. p. V001T03A003, 2017.
- [14] P. Guillot, A. Colin, and A. Ajdari, "Stability of a jet in confined pressure-driven biphasic flows at low Reynolds number in various geometries," *Phys. Rev. E Stat. Nonlinear, Soft Matter Phys.*, vol. 78, no. 1, 2008.
- [15] P. Guillot, A. Colin, A. S. Utada, and A. Ajdari, "Stability of a Jet in Confined Pressure-Driven Biphasic Flows at Low Reynolds Numbers," *Phys. Rev. Lett.*, vol. 99, no. 10, p. 104502, Sep. 2007.
- [16] M. A. Herrada, A. M. Gañán-Calvo, and P. Guillot, "Spatiotemporal instability of a confined capillary jet," *Phys. Rev. E Stat. Nonlinear, Soft Matter Phys.*, vol. 78, no. 4, pp. 1–7, 2008.

- [17] K. J. Humphry, A. Ajdari, A. Fernández-Nieves, H. A. Stone, and D. A. Weitz, "Suppression of instabilities in multiphase flow by geometric confinement," *Phys. Rev. E Stat. Nonlinear, Soft Matter Phys.*, vol. 79, no. 5, pp. 1–5, 2009.
- [18] M. L. Cordero, F. Gallaire, and C. N. Baroud, "Quantitative analysis of the dripping and jetting regimes in co-flowing capillary jets," *Phys. Fluids*, vol. 23, no. 9, 2011.
- [19] J. M. Gordillo, A. Sevilla, and F. Campo-Cortés, "Global stability of stretched jets: conditions for the generation of monodisperse micro-emulsions using coflows," *J. Fluid Mech.*, vol. 738, pp. 335–357, 2014.
- [20] A. Gañán-Calvo, "Generation of Steady Liquid Microthreads and Micron-Sized Monodisperse Sprays in Gas Streams," *Phys. Rev. Lett.*, vol. 80, no. 2, pp. 285–288, 1998.
- [21] C. N. Baroud, F. Gallaire, and R. Dangla, "Dynamics of microfluidic droplets.," *Lab Chip*, vol. 10, pp. 2032–2045, 2010.
- [22] A. S. Utada, A. Fernandez-Nieves, H. A. Stone, and D. A. Weitz, "Dripping to jetting transitions in coflowing liquid streams," *Phys. Rev. Lett.*, vol. 99, no. 9, pp. 1–4, 2007.
- [23] Lord Rayleigh, "On the Instability of Jets," *Proc. London Math. Soc.*, vol. 10, no. June 1873, pp. 4–13, 1878
- [24] M. Wörner, "Numerical modeling of multiphase flows in microfluidics and micro process engineering: A review of methods and applications," *Microfluid. Nanofluidics*, vol. 12, no. 6, pp. 841–886, 2012.
- [25] E. Olsson and G. Kreiss, "A conservative level set method for two phase flow," *J. Comput. Phys.*, vol. 210, no. 1, pp. 225–246, 2005.
- [26] J. U. Brackbill, D. B. Kothe, and C. Zemach, "A continuum method for modeling surface tension," *J. Comput. Phys.*, vol. 100, no. 2, pp. 335–354, 1992.